(16) Wilkinson, M. K.; Gaunt, D. S.; Lipson, J. E. G.; Whittington, S. G. *J. Phys. A* **1986**, *19*, 789.
(17) Whittington, S. G.; Lipson, J. E. G.; Wilkinson, M. K.; Gaunt, D. S. *Macromolecules* **1986**, *19*, 1241.
(18) Barrett, A. J.; Pound, A. *J. Phys. A* **1980**, *13*, 1811.
(19) LeGuillou, J. C.; Zinn-Justin, J. *Phys. Rev. B* **1980**, *21*, 3976.
(20) de Gennes, P. G. *Scaling Concepts in Polymer Physics*: Cornell: Ithaca, NY, 1979.
(21) Torrie, G.; Whittington, S. G. *J. Phys. A* **1975**, *8*, 1178; **1977**, *10*, 1345.
(22) Rosenbluth, M.; Rosenbluth, A. W. *J. Chem. Phys.* **1955**, *23*, 356.
(23) Igloi, F. *J. Phys. A* **1986**, *19*, 3077.
(24) Gaunt, D. S.; Guttmann, A. J. In *Phase Transitions and Critical Phenomena*; Domb, C., Green, M. S., Eds; Academic: New York, 1974; Vol. 3, Chapter 4.
(25) Domb, C. *J. Chem. Phys.* **1963**, *38*, 2957.
(26) Rapaport, D. C. *J. Phys. A* **1985**, *18*, 113.
(27) Nielsen, K. L. *Methods in Numerical Analysis*; Macmillan: New York, 1956.

Configuration of Terminally Attached Chains at the Solid/Solvent Interface: Self-Consistent Field Theory and a Monte Carlo Model

Terence Cosgrove* and Timothy Heath

School of Chemistry, University of Bristol, Bristol BS8 1TS, U.K.

Boudewijn van Lent, Frans Leermakers, and Jan Scheutjens

Laboratory for Physical and Colloid Chemistry, Agricultural University, De Dreijen 6, 6703 BC Wageningen, The Netherlands. *Received August 26, 1986*

ABSTRACT: Segment density distributions, root mean square (rms) thicknesses, and bound fractions have been calculated for terminally attached chains at the solid/solvent interface. The effects of coverage, solvent quality, and adsorption energy are considered. Both the self-consistent field theory of Scheutjens and Fleer and a Monte Carlo method have been used. The results show a marked difference between systems with adsorption energies above and below the cricital value. Solvency has a significant effect on the variation of the rms thickness with chain length. At high coverages, polymer configurations with small bound fractions and highly extended tails are found. Differences between the two models are discussed.

Introduction

The configuration of terminally attached polymers at the solid/solvent interface has attracted a great deal of interest both experimentally and theoretically.[1] This interest is in-line with the increased use of these polymers as dispersion stabilizers, adhesives, etc. Experimentally, only small-angle neutron scattering[2] (SANS) has been used successfully to measure the segment density distribution of a terminally attached polymer at the solid/solvent interface.[3,4] The data for terminally attached polystyrene on silica in carbon tetrachloride[4] showed a clear maximum in the density distribution away from the interface. This could be interpreted in terms of a low χ_s[1,4] (the difference in the energy of adsorption of a segment and a solvent molecule in units of kT) and a high grafted amount. For physically adsorbed polystyrene on silica, however, a monotonically decreasing density distribution was found.

Theoretically, a large number of different approaches have been used to describe these systems. These can be divided into isolated chain[5-7] and interacting chain models.[8-10] Some of these models have used a lattice to constrain the number of chain conformations generated. An advantage of a lattice model is that the energy originating from nearest-neighbor interactions can easily be calculated.

For a single terminally attached chain, Hesselink[5] has given an analytical form for the density distribution, but no account is taken of the solvent or surface interactions. In the exact enumeration self-avoiding walk procedure,[6] the surface interaction is included and the critical adsorption energy χ_{sc} was determined. Croxton[7] has developed a self-avoiding hard-sphere model for terminally attached chains not constrained by a lattice. A monotonically decreasing segment density profile is found at high χ_s, whereas a profile with a pronounced maximum is found at low χ_s. The profiles however show a marked discontinuity near the interface.

For chemically grafted chains, there are often high chain densities at the interface, and single-chain models are unsatisfactory. Hesselink,[5] de Gennes,[10] and Dolan and Edwards[8] have discussed the influence of lateral interactions between chains. However, they have only considered the case for $\chi_s = 0$. Levine et al.[9] have combined the self-consistent field approximation with the matrix representation method of DiMarzio and Rubin.[11] In their paper, they calculate segment density profiles for terminally attached chains between two plates for different values of χ_s. They do not give any data for a single surface or a breakdown of the distribution in terms of segments in trains and loops. Clark and Lal[12] have used the Monte Carlo method with the periodic boundary constraint to mimic the effect of coverage. In their simulation, they generate new chain conformations from a parent distribution by a four-bond rotation; only the good solvent case is considered.

In this paper we compare a Monte Carlo approach with that of the Scheutjens–Fleer lattice model, extended to the case of terminally attached chains.

Monte Carlo Simulation

The Monte Carlo simulation for terminally attached chains was carried out by generating a large sample of self-avoiding walks on a simple cubic lattice. The surface was taken as a plane which the walks cannot cross. The first segment was attached at the origin (i,j,k = 1,0,0). At each point on the walk, the surrounding lattice sites were tested for previous visits before the next step was generated. The probability of making a step to any adjacent free site depends on the number of free sites available.[13] For example, in an "open" walk, where five of the surrounding positions are free, the probability of a step is $^1/_5$. In a "compact" walk, where, say, only two adjacent sites

* To whom all correspondence should be addressed.

0024-9297/87/2220-1692$01.50/0 © 1987 American Chemical Society

are free, the probability is $^1/_2$. Clearly, the more compact walks are more probable, and each walk must, therefore, be weighted by the reciprocal of the product of the probabilities of the individual steps taken.

As a walk was generated, the number of segment–segment contacts was counted, assuming only nearest-neighbor interactions. Hence, the number of contacts between polymer segments (p) and solvent molecules (s), $n_{p,s}$, could be obtained and each conformation weighted by the factor $\exp(-\chi n_{p,s}/z)$, where z is the coordination number of the lattice and χ is the Flory–Huggins parameter defined as the net enthalpy change per z segment–solvent contacts created on mixing pure solvent and polymer. Similarly, the interactions of the polymer with the surface were included by weighting with the factor $\exp(n_1\chi_s)$, where n_1 is the number of segments the conformation has in the first layer.

The effect of coverage was introduced by placing periodic boundaries[12] at various distances, b, from the origin such that a walk reaching $j = b$ or $k = b$ could step through the boundary but reappear at $(i,-b,k)$ or $(i,j,-b)$, respectively. Each walk was therefore generated in the environment of identical surrounding walks.

Samples of 200 000 walks were taken, for chains of 50 segments.

Mean Field Theory

The Scheutjens–Fleer polymer adsorption theory,[15,16] a lattice theory using an extension of the Flory–Huggins model for an inhomogeneous system, can be modified in a quite straightforward manner for the case of terminally attached chains. In this lattice there are M layers numbered sequentially from the surface. Each layer has L sites. A lattice site has z nearest neighbors, of which a fraction, λ_0, are in the same layer and a fraction, λ_1, are in each of the adjacent layers. Every lattice site can accomodate either a solvent molecule or a polymer segment. The volume fractions in each layer are defined as $\phi_i = n_i/L$ and $\phi_i^0 = n_i^0/L$, where n_i and n_i^0 are the number of segments and solvent molecules in layer i, respectively.

Scheutjens and Fleer calculate the probability of every conformation on this lattice. They define a conformation as the sequence of layers in which the successive segments of a chain are situated. Lateral interactions are accounted for in a mean field approximation. Each segment in a given layer, i, has the same interaction energy, dependent on the volume fractions in layers $i-1$, i, and $i+1$, the lattice parameters λ_0 and λ_1, χ_s (if $i = 1$), and χ. The total polymer–solvent interaction energy, u_{int}, in the lattice is given by[15]

$$u_{int} = kT\chi\sum_{i=1}^{M} n_i^0\langle\phi_i\rangle \tag{1}$$

The site volume fraction, $\langle\phi_i\rangle$, is defined as

$$\langle\phi_i\rangle = \lambda_1\phi_{i-1} + \lambda_0\phi_i + \lambda_1\phi_{i+1} \tag{2}$$

The adsorption energy is calculated as

$$u_{ads} = -kTn_1\chi_s \tag{3}$$

A very important parameter in the theory is the free segment probability, P_i. P_i determines the probability of finding a free segment (monomer) in layer i. The equation for P_i is derived from the partition function and is given by

$$P_i = \phi_i^0 e^{\chi(\langle\phi_i\rangle - \langle\phi_i^0\rangle)} e^{\chi_s\delta(1,i)} \tag{4}$$

The Kronecker delta, $\delta(1,i)$, equals unity for $i = 1$ and zero for $i \neq 1$.

The end segment probability, $P(i,r)$, i.e., the probability that the end segment of a chain of r segments is in layer i, is calculated from P_i by using the matrix method of DiMarzio and Rubin.[11] For every value of i,

$$P(i,r) = P_i[\lambda_1 P(i-1,r-1) + \lambda_0 P(i,r-1) + \lambda_1 P(i+1,r-1)] \tag{5}$$

$P(i,r)$ is therefore expressed in the end segment probabilities of chains which are one segment shorter. In the same way, the end segment probability of a chain of $(r-1)$ segments depends on the end segment probabilities of a chain of $(r-2)$ segments, etc. Ultimately, $P(i,r)$ for each i can be written as a function of all the $P(i,1)$, where the "end" segment probability, $P(i,1)$, for a monomer equals P_i:

$$\begin{bmatrix} P(1,r) \\ \cdot \\ \cdot \\ P(i,r) \\ \cdot \\ \cdot \\ P(M,r) \end{bmatrix} = \begin{bmatrix} \lambda_0 P_1 & \lambda_1 P_1 & 0 & & & & 0 \\ \lambda_1 P_2 & \cdot & \cdot & & & & \\ 0 & \cdot & \cdot & \cdot & & & \\ & & \lambda_1 P_i & \lambda_0 P_i & \lambda_1 P_i & & \\ & & & \cdot & \cdot & \cdot & 0 \\ & & & & \cdot & \cdot & \lambda_1 P_{M-1} \\ 0 & & & & 0 & \lambda_1 P_M & \lambda_0 P_M \end{bmatrix}^{r-1} \begin{bmatrix} P_1 \\ \cdot \\ \cdot \\ P_i \\ \cdot \\ \cdot \\ P_M \end{bmatrix} \tag{6}$$

which can be written as

$$\mathbf{P}(r) = \mathbf{W}^{r-1}\mathbf{P}(1) \tag{7}$$

where $\mathbf{P}(1)$ contains the elements $P(i,1)$ which equal P_i for chains that are not terminally attached. This matrix method gives a set of end segment probabilities, which can be arranged in matrix form:

$$\mathbf{P} = \begin{bmatrix} P(1,1) & \cdots & P(1,s) & \cdots & P(1,r) \\ \cdot & \cdots & \cdot & \cdots & \cdot \\ \cdot & \cdots & \cdot & \cdots & \cdot \\ P(i,1) & \cdots & P(i,s) & \cdots & P(i,r) \\ \cdot & \cdots & \cdot & \cdots & \cdot \\ \cdot & \cdots & \cdot & \cdots & \cdot \\ P(M,1) & \cdots & P(M,s) & \cdots & P(M,r) \end{bmatrix} \tag{8}$$

For terminally attached (ta) chains, the end segment probabilities must be modified. The first segment is constrained to be in layer 1, so the first column of matrix 8 is simplified to

$$\mathbf{P}_{ta}(1) = \begin{bmatrix} P_1 \\ 0 \\ \cdot \\ \cdot \\ \cdot \\ \cdot \\ 0 \end{bmatrix} \tag{9}$$

If we carry out the matrix multiplications, we obtain

$$\mathbf{P}_{ta} = \begin{bmatrix} P_1 & P_{ta}(1,2) & \cdots & P_{ta}(1,s) & \cdots & P_{ta}(1,r) \\ 0 & P_{ta}(2,2) & \cdots & \cdot & \cdots & \cdot \\ & & \cdots & P_{ta}(i,s) & \cdots & P_{ta}(i,r) \\ & & \cdots & \cdot & \cdots & \cdot \\ 0 & & & 0 & P_{ta}(M,s) & \cdots & P_{ta}(M,r) \end{bmatrix} \tag{10}$$

Scheutjens and Fleer have shown that it is possible to calculate $\phi_i(s)$, the volume fraction due to segment s in layer i, through the formula

$$\phi_i(s) = \frac{\theta}{rP_{ta}(r)} P_{ta}(i,s;r) \tag{11}$$

θ is the total grafted amount (in equivalent monolayers),

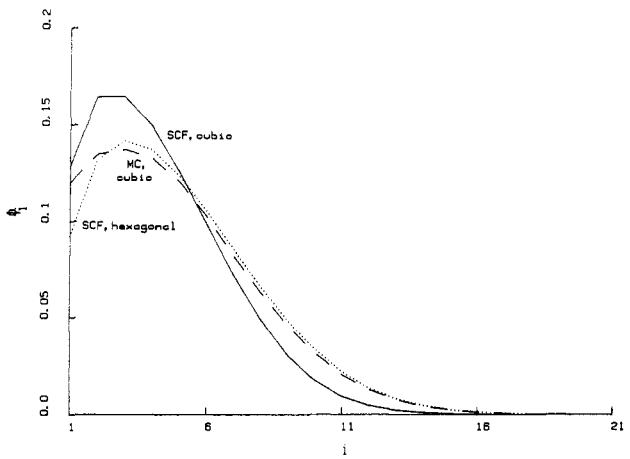

Figure 1. Volume fraction ϕ_i as a function of layer number i for a constant value of θ (1.02). The MC calculations (- - -) are for a cubic lattice, $\lambda_0 = {}^2/_3$, while the SCF calculations are for a cubic (—) and hexagonal lattice (···), $\lambda_0 = {}^1/_2$. Data are shown for r = 50, $\chi_s = 0$, and $\chi = 0.4$.

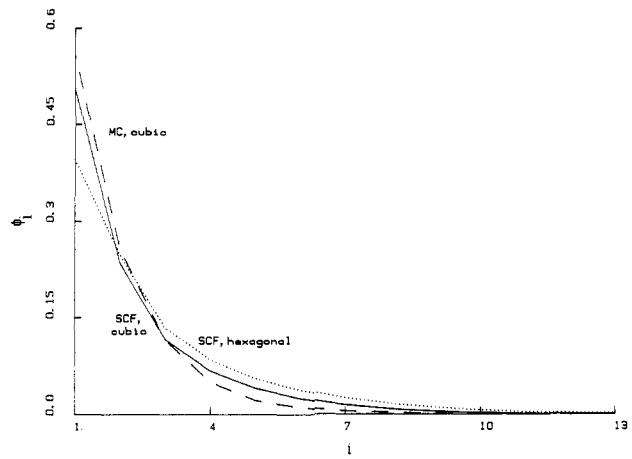

Figure 2. Volume fraction ϕ_i as a function of layer number i. All parameters are the same as in Figure 1, except for χ_s, which equals 0.6. (- - -) MC, $\lambda_0 = {}^2/_3$; (—) SCF, $\lambda_0 = {}^2/_3$; (···) SCF, $\lambda_0 = {}^1/_2$.

which equals $\sum_i \phi_i$, and $P_{ta}(r)$ is the sum over the components of the last column of matrix 10: $P_{ta}(r) = \sum_i P_{ta}(i,r)$. $P_{ta}(i,s;r)$ is the probability of finding the sth segment of a terminally attached r-mer in layer i. It can be calculated by joining a terminally attached chain of s segments and a non-terminally attached chain of $(r - s + 1)$ segments. This gives

$$P_{ta}(i,s;r) = \frac{P_{ta}(i,s)P(i,r-s+1)}{P_i} \tag{12}$$

$P_{ta}(i,s)$ is obtained from matrix 10 and $P(i,r-s+1)$ from matrix 8.

Combining eq 11 and 12 and summing over s gives

$$\phi_i = \frac{\theta}{rP_{ta}(r)} \sum_{s=1}^{r} \frac{P_{ta}(i,s)P(i,r-s+1)}{P_i} \tag{13}$$

Scheutjens and Fleer have shown that ϕ_i and P_i can be calculated numerically, using eq 13 and 4 and the boundary condition $\phi_i + \phi_i^0 = 1$.

The profiles due to loops and tails can be calculated by using the same procedure as eq 23 and 24 of ref 16. The tail profile is given by

$$\phi_i^t = \frac{\theta}{rP_{ta}(r)} \sum_{s=2}^{r} \frac{P_{ta}(i,s)P_f(i,r-s+1)}{P_i} \quad (i > 1) \tag{14}$$

where $P_f(i,r-s+1)$ is the end segment probability of a "free chain"; i.e., it has no segments in the first layer. This can be found by putting $P_1 = 0$ in eq 6; hence, $P_f(1,s) = 0$ for every s. Therefore, the elements of the first row in matrix 8 equal zero for a free chain. Moreover, $P_f(i,s) < P(i,s)$ for $i \leq s$.

The volume fraction in layer i due to segments in loops can be calculated by using an equation similar to eq 14:

$$\phi_i^l = \frac{\theta}{rP_{ta}(r)} \sum_{s=2}^{r-1} \frac{P_{ta}(i,s)P_a(i,r-s+1)}{P_i} \quad (i > 1) \tag{15}$$

$P_a(i,r-s+1)$ is the end segment probability of a (non-terminally attached) chain which has at least one segment in layer 1. It is defined as[16]

$$P_a(i,r-s+1) = P(i,r-s+1) - P_f(i,r-s+1)$$

Results and Discussion

In Figures 1 and 2 we show concentration profiles for terminally attached chains of 50 segments for $\theta = 1.02$, $\chi = 0.4$, and two values of χ_s. The profiles have been calculated by using both the self-consistent field (SCF) theory, for hexagonal and cubic lattices, and the Monte Carlo (MC) method on the cubic lattice. In Figure 1, χ_s is below the critical value and the profiles show a definite maximum away from the interface. The choice of parameters has been made to best simulate the experimental data in ref 3. Qualitatively the agreement is rather good. For $\chi_s = 0$, the profiles are also similar in shape to those predicted by Hesselink[5] and Dolan and Edwards[8] but do not show the discontinuities found by Croxton.[7] In Figure 2, χ_s is greater than the critical value and the profiles fall monotonically, in-line with the experimental results of ref 4.

Qualitatively, both the MC and SCF profiles are similar, though there are systematic differences. Comparing the SCF and MC profiles on the cubic lattice for $\chi_s = 0$ (Figure 1), we see that the MC profile extends slightly further into the bulk. This may be attributed to the effect of excluded volume, which is accounted for explicitly in the MC model but only through the Bragg–Williams approximation in the SCF theory. The effect is more pronounced at larger values of θ. For the $\chi_s = 0.6$ case, the MC model predicts a higher segment volume fraction in the first layer than the SCF theory. This is because the initial steps on the lattice are not weighted by the presence of later segments in the walk (an artifact of the periodic boundary condition in the MC model). This effect becomes more important when the segment volume fractions close to the surface are large. In the SCF theory, however, the free segment probability in each layer is weighted by the average volume fraction in that layer, which is not unreasonable when the points of attachment are randomly distributed.

In Figures 1 and 2, the influence of the lattice on the SCF profiles is also shown. For the cubic lattice ($\lambda_0 = {}^2/_3$) there is a much greater probability that a chain will stay in the same layer than cross into an adjacent layer. This will have the effect of compressing the profile and increasing the value of p, the fraction of segments in the first layer.

In Figure 3, we show the decomposition of the SCF profiles into loops and tails, in a good solvent, for two values of χ_s at a fixed θ of 1. For $\chi_s = 0$, there is a larger fraction of segments in tails compared to that for $\chi_s = 1$, the reverse being true for loops. The p value in the latter case is also higher (see Figure 5). For $\chi_s = 0$, there are still a significant number of segments in trains and loops, and this is due to the short chain lengths in this simulation. As the chain length increases, then p should vary as $1/r$.

In Figure 4, we show profiles for a chain length of 250, $\theta = 10$, and values for χ_s of 0 and 1. Only the SCF results

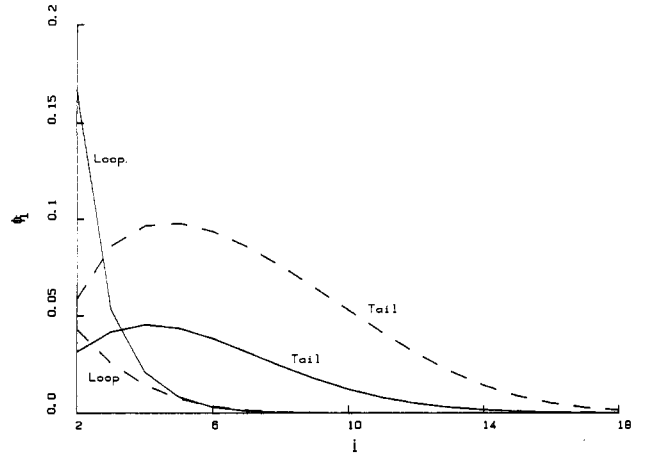

Figure 3. Volume fraction of loops and tails as a function of layer number i for two different values of χ_s, in a good solvent. SCF theory. $\chi_s = 0$ (- - -) and $\chi_s = 1$ (—); $\chi = 0$; $r = 50$; $\theta = 1$; $\lambda_0 = {}^1/_2$.

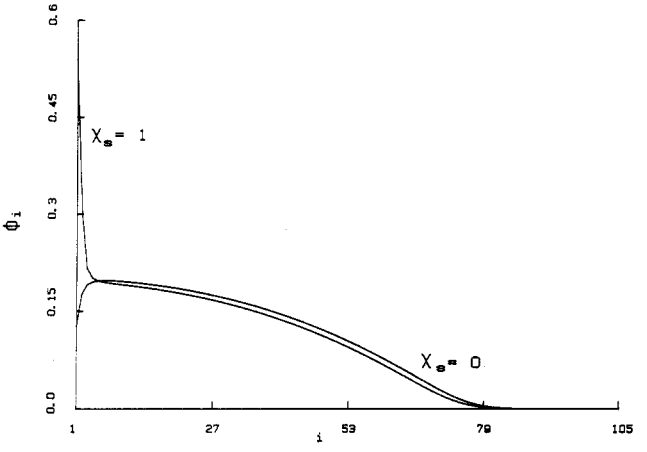

Figure 4. Volume fraction ϕ_i as a function of layer number i. $\chi_s = 0$ (- - -), $\chi_s = 1$ (—). Grafted amount $\theta = 10$; $r = 250$.

have been calculated because of the large computation times required for MC. For $\chi_s = 0$, the profile is similar to the profile in Figure 1 except that the segments reach further into solution. The profile however does show a region of almost constant density as predicted by de Gennes[10]. The volume fraction in this region obeys the mean-field prediction $(\theta/r)^{1/2}$, which is 0.2, in this case. Scaling[10] predicts a volume fraction of $(\theta/r)^{2/3}$, which would be 0.12.

In Figures 5 and 6, the variation of p and t_{rms} (root mean square thickness) for $r = 150$ is shown as a function of grafted amount, using the SCF theory. As expected, with increasing χ_s for a given value of θ, p increases, whereas t_{rms} decreases. With increasing θ but fixed $\chi_s > \chi_{sc}$, t_{rms} increases and p decreases. For $\chi_s = 0$, the p values show a very weak maximum (which is not visible in the diagram). Unlike physical adsorption from bulk solution, θ can be varied independently of χ_s; the values of θ used here cannot be achieved by physical adsorption from solution. MC calculations show the same general trends as the SCF theory for both p and t_{rms}.

Finally, in Figure 7 we show the variation in t_{rms} for a fixed grafted amount ($\theta = 1$), in a good and in a theta solvent, as a function of chain length. Note that, since θ is fixed, the surface area per chain increases linearly with chain length. For a theta solvent and $\chi_s = 1$, t_{rms} is virtually independent of chain length. The chains prefer to stay in the concentrated region near the interface, and the formation of extended tails is suppressed. In both good and poor solvents with $\chi_s = 0$, t_{rms} increases with increasing chain length.

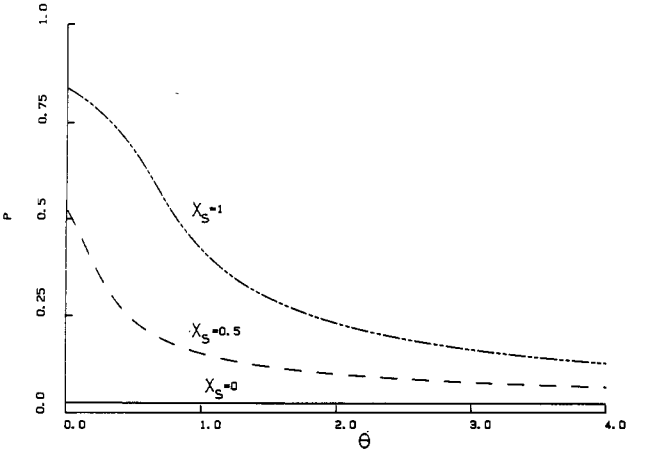

Figure 5. Variation of the bound fraction p with the grafted amount θ for three different values of χ_s, in a good solvent. SCF theory. $\chi_s = 0$ (—), $\chi_s = 0.5$ (- - -), and $\chi_s = 1$ (-·-·-); $\chi = 0$; $r = 150$; $\lambda_0 = {}^1/_2$.

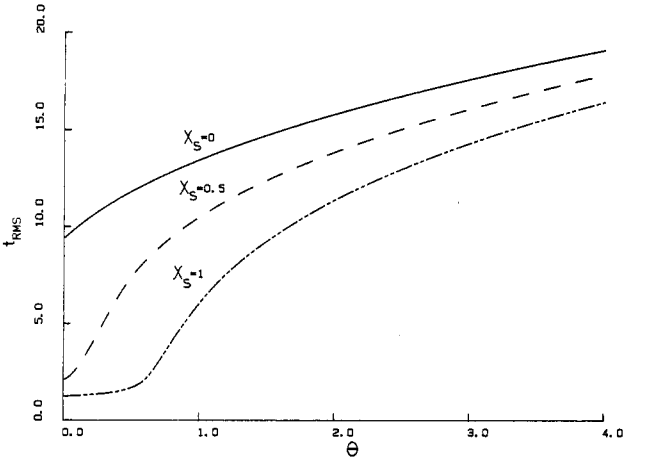

Figure 6. Root mean square layer thickness t_{rms} as a function of the grafted amount θ for three different values of χ_s, in a good solvent. SCF theory. $\chi_s = 0$ (—), $\chi_s = 0.5$ (- - -), and $\chi_s = 1$ (-·-·-); $\chi = 0$; $r = 150$; $\lambda_0 = {}^1/_2$.

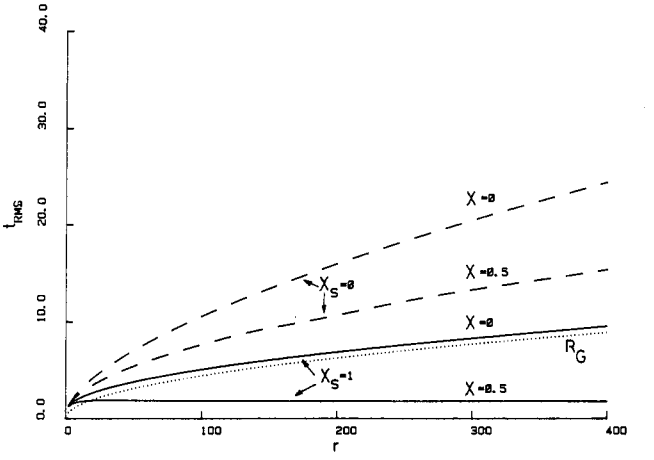

Figure 7. Root mean square layer thickness t_{rms} as a function of the chain length r for two different values of χ_s, in a good ($\chi = 0$) and in a theta solvent ($\chi = 0.5$). SCF theory. $\chi_s = 0$ (- - -) and $\chi_s = 1$ (—); $\theta = 1$; $\lambda_0 = {}^1/_2$. Also the radius of gyration R_G as a function of r is shown (···).

The radius of gyration, R_G, of a free chain in a theta solvent is given by[17]

$$R_G^2 = (r/6)(1 + z^{-1})/(1 - z^{-1}) \qquad (16)$$

For comparison, the variation of R_G with chain length is also plotted in Figure 7 (dotted curve). Except for $\chi_s = 1$ and $\chi = 0.5$, t_{rms} appears to be larger than R_G. This is in contrast to physically adsorbing chains from solution, in which case t_{rms} is usually smaller than R_G.[16] For $\chi_s = 0$ and $\chi = 0$, t_{rms} is approximately $2.5R_G$. This emphasizes that terminally attached chains can form highly extended layers in comparison with purely physically adsorbed chains from solution.

Conclusion

Both MC and SCF calculations of terminally attached chains predict similar adsorption profiles. Small differences have been accounted for in terms of excluded volume effects and the periodic boundary condition. At high grafted amounts and for low χ_s, highly extended adsorbed layers are formed, emphasizing the usefulness of these systems as steric stabilizers.

Acknowledgment. We thank B. Vincent and G. J. Fleer for their interest and encouragement during this project. T. Cosgrove thanks G. J. Fleer for arranging a short stay in Wageningen where this work was first envisaged. B. v. Lent thanks T. Cosgrove for arranging a stay in Bristol where this work was completed.

References and Notes

(1) Cosgrove, T.; Cohen Stuart, M.; Vincent, B. *Adv. Colloid Interface Sci.* **1985**, *24*, 81.
(2) Crowley, T. L. Ph.D. Thesis, Oxford, 1984.
(3) Cosgrove, T.; Crowley, T. L.; Vincent, B. In *Adsorption from Solution*; Rochester, C. H., Ottewill, R. H., Eds.; Academic: New York, 1983; p 283.
(4) Cosgrove, T.; Heath, T. G.; Ryan, K.; van Lent, B. *Polymer* **1987**, *28*, 64.
(5) Hesselink, F. Th. *J. Chem. Phys.* **1964**, *73*, 3488.
(6) Cosgrove, T. *Macromolecules* **1982**, *15*, 1290.
(7) Croxton, C. *J. Phys. A* **1983**, *16*, 4343.
(8) Dolan, A. K.; Edwards, S. F. *Proc. R. Soc. London, Ser. A* **1975**, *A343*, 427.
(9) Levine, S.; Thomlinson, M. M.; Robinson, K. *Faraday Discuss.* **1978**, *65*, 202.
(10) de Gennes, P. G. *Macromolecules* **1980**, *13*, 1069.
(11) DiMarzio, E. A.; Rubin, R. J. *J. Chem. Phys.* **1971**, *55*, 4318.
(12) Clark, A. T.; Lal, M. *J. Chem. Soc., Faraday Trans. 2* **1975**, *74*, 1857.
(13) Rosenbluth, M. N.; Rosenbluth, A. W. *J. Chem. Phys.* **1955**, *23*, 356.
(14) Silberberg, A. *J. Chem. Phys.* **1968**, *48*, 2835.
(15) Scheutjens, J. M. H. M.; Fleer, G. J. *J. Phys. Chem.* **1979**, *83*, 1619.
(16) Scheutjens, J. M. H. M.; Fleer, G. J. *J. Phys. Chem.* **1980**, *84*, 178.
(17) Yamakawa, H. In *Modern Theory of Polymer Solutions*; Harper and Row: New York, 1971; p 124.

Osmotic Compressibility and Mechanical Moduli of Swollen Polymeric Networks

Ivet Bahar and Burak Erman*

School of Engineering, Boğaziçi University, 80815 Bebek, Istanbul, Turkey.
Received November 12, 1986

ABSTRACT: The thermodynamics of polymeric networks subject to the action of a solvent is reviewed. Expressions for the osmotic compressibility and elastic moduli (bulk and shear) of the swollen network are derived in relation to the molecular characteristics of the system. The dependence of the osmotic compressibility on the equilibrium degree of swelling and the solvent quality is investigated. A strong dependence of osmotic compressibility on the nature of the solvent is emphasized. Predictions of the theory are compared with scaling arguments and results of experiments on swollen PVAc networks.

I. Introduction

Early studies of the degree of swelling of networks exposed to a solvent were made on butyl[1] and natural rubbers[2] under uniaxial tension and on natural rubber[3,4] in uniaxial tension, compression, and equibiaxial extension. The relationship of the volume changes to elongation in poly(dimethylsiloxane) networks in uniaxial extension[5] was analyzed at different solvent activities. More recently, the mechanical behavior of swollen polymer networks was analyzed by experiments such as dynamic (quasi-elastic) light scattering, osmotic deswelling, and uniaxial compression.[6,7]

Interpretation of results of the experiments outlined above may suitably be made by thermodynamic arguments that rest on the proper representation of the total free energy of the network–solvent system. In the present study, the thermodynamics of network–solvent systems are reviewed, with particular emphasis on the formulation of the osmotic compressibility and elastic modulus in terms of solution properties and network constitution.

In section II, the general thermodynamic formulation is presented. The total free energy is assumed to be the sum of the free energy of mixing and the elastic free energy of the network. The solvent chemical potential, the osmotic compressibility, and the elastic moduli (bulk and shear) of the swollen network are derived.

In section III, the dependence of the osmotic compressibility on the equilibrium degree of swelling and on the χ-parameter is explored. In many real systems, departures from a regular solution are attributed to the concentration dependence of the polymer–solvent interaction parameter which plays a major role in critical transitions. It is shown that for a unique value of the concentration-dependent χ-parameter critical conditions may indeed result, leading to infinite osmotic compressibility. In section IV, the theoretically predicted osmotic compressibility and the elastic modulus of a swollen network are compared with experimental data. The present theory, which basically parallels the treatment of ref 1–5, is compared in the last section with recent scaling arguments.

II. General Formulation

Deformation of Swollen Networks. The state of deformation in a polymeric network under stress may be decomposed into a dilation and a distortion term as[8]

$$\lambda = (\mathbf{v}_2^0/v_2)^{1/3}\alpha = (V/V^0)^{1/3}\alpha \qquad (1)$$

Here v_2^0 is the volume fraction of the polymer during

0024-9297/87/2220-1696$01.50/0 © 1987 American Chemical Society